

# Performance Insights on IEEE 802.11a/g Compliant Software-based In-Band Full Duplex Relay Systems

Muhammad Sohaib Amjad and Falko Dressler

Heinz Nixdorf Institute and Dept. of Computer Science, Paderborn University, Germany

{amjad,dressler}@ccs-labs.org

**Abstract**—Over the last decade, infrastructure relays have been employed by wireless standards, such as WiMAX and LTE, for coverage and performance enhancement. However, due to their Half-Duplex (HD) nature, these relays incur spectral losses and increase the end-to-end delay. In contrast, in-band Full-Duplex (FD) relays can effectively cope with these issues through simultaneous reception and forwarding, provided that the looped-back Self-Interference (SI) is sufficiently suppressed. Driven by the possible performance gain of FD relaying over traditional HD relay systems; in this work, we present the first implementation of IEEE 802.11a/g compliant FD relay system in GNU Radio framework. Given the Open Source nature of this real-time signal processing software, the implementation is completely transparent and can be studied in all details and modified if needed. For a holistic evaluation of our relay system, we implemented both Amplify and Forward (AF) and Decode and Forward (DF), the two widely adopted relaying strategies. We assess the performance of these relaying strategies both analytically and in simulation experiments. Our results demonstrate and underline the potential gains of full-duplex relays in-terms of spectral efficiency and end-to-end physical layer latency over traditional half-duplex relay systems.

## I. INTRODUCTION

The highly complex and unpredictable nature of a wireless channel poses critical challenges for reliable high-speed communication. The susceptibility of a radio signal to noise, interference, and other channel impairments, which can also vary over time, has a significant impact on the overall performance. To achieve reliable communication in severe channel conditions, both channel capacity (achievable data rate) and coverage area need to be traded off, i.e., to improve one, the other needs to be compromised. In recent years, to overcome this channel capacity vs. coverage dilemma, infrastructure relays have been used, and even incorporated in wireless standards like 3GPP LTE [1] and WiMAX [2], as they can greatly enhance the capacity gains, and extend the coverage of a wireless system at the same time.

Nevertheless, these relays operate in Half-Duplex (HD) mode, and since they can not simultaneously receive and transmit, they require additional resources typically in time domain for reliable communication. In a classical two-hop relay system, a relay node is introduced between source and destination nodes. The task of relay node is to receive the signal from source in the first time slot, and forward it towards destination in the next possible time slot, where the waiting time before forwarding depends on the implemented relaying protocol. These traditional relays with HD-based architecture,

not only introduce spectral losses, but their deployment in the system also increases the overall latency.

In the past few years, in-band Full-Duplex (FD) wireless systems have gained significant attention, and a substantial amount of research has been done in the area [3]. In an effort to recover the spectral losses, and to improve the capacity gain of classical HD systems through in-band FD communications, the advances in signal processing capability and antenna technology have played a key role. Several works [4]–[7] have presented different techniques and architectures to address the prime factor impeding in-band FD communications, i.e., the Self-Interference (SI), which fundamentally arises due to radio’s own transmission at the same time and frequency.

A relay system with in-band full-duplex transmission capability can simultaneously receive from a source, and transmit towards a destination. This not only reduces the latency of a multi-hop relay system but it also improves the spectral efficiency. However, for optimal performance, suppression of Looped Self-Interference (LSI) to the receiver’s noise floor is a critical requirement in a Full-Duplex Relay (FDR) system. Any residual LSI basically worsens the noise floor for the Signal-of-Interest (SoI), resulting in poor Signal-to-Noise Ratio (SNR), which reduces the overall system performance.

In this work, we first model Amplify and Forward (AF) and Decode and Forward (DF) relaying strategies in both HD and FD modes for a dual-hop scenario, i.e., source-relay-destination, and obtain the closed-form expressions of received SNR at both relay and destination ends. We, then present the performance results with our software-based implementation of both HD and FD based AF and DF relay systems. We implement the system in GNU Radio<sup>1</sup>, a real-time signal processing framework for simulation and experimental evaluation. We further analyze the performance of these relaying systems in-terms of Packet Delivery Ratio (PDR), achievable spectral efficiency, and Physical Layer Latency (PLL) with the open source stack for IEEE 802.11a/g/p WLAN developed by Bloessl et al. [8], [9]. To the best of our knowledge, this is the first work which evaluates the performance of FD relaying system with a General Purpose Processor (GPP)-based software implementation of the IEEE 802.11a/g WLAN standard. Our evaluation results demonstrate and underline the potential performance gains offered by FD relays, in particular with DF relaying strategy, over HD relay systems.

<sup>1</sup><https://www.gnuradio.org/>

Our main contributions can be summarized as follows:

- We analytically model both AF and DF relaying strategies in HD and FD transmission modes, and obtain closed-form expressions, to numerically study the impact of amplification factor and estimation error in SI channel on the received SNR.
- We implement an FDR system that includes a novel core module for LSI cancellation in GNU Radio, a GPP-based open-source signal processing framework. This makes the implementation accessible to fellow researchers and allows easy modifications for the testing of new concepts.
- For the first time, we evaluate and compare the performance of IEEE 802.11a/g compliant Half-Duplex Relays (HDRs) with emerging FDR systems, and present an extensive-set of performance results for frequency selective Rayleigh fading channels.
- Comparing the AF and DF relaying strategies in full-duplex mode, we show that under same channel conditions DF strategy outperforms AF relaying by 6 dB–7 dB and, therefore, yields better spectral efficiency and lower physical layer latency.

## II. RELATED WORK

In the era of ever growing wireless traffic and high speed connectivity, multi-hop communication via relay nodes has emerged as an attractive solution to enhance the coverage and capacity of a band-limited wireless link. In the literature, to overcome the added disadvantages of these relaying strategies due their half-duplex nature, different works have considered approaches such as cooperative decoding for diversity gain [10], and two alternating relay nodes to mimic FD mode [11]. Nevertheless, these approaches have not been able to entirely compensate for the losses these HD relays incur.

Recently, full-duplex relaying has gained significant attention. After-all, its implications are qualitatively beneficial in terms of both spectral efficiency and network latency. However, most of the research conducted in this context is focused on analytical findings and theoretical approaches to state the gains of FD relaying. For example, [12] analytically models LSI and quantization noise to analyze the achievable spectral efficiency. Similarly, [13] studies Markov chain based models to analyze the outage probability in FD multi-relay channels. Likewise, [14] investigates the impact of looped back channel estimation error on the performance of AF based FD relaying. In [15], the optimal power allocation in DF based FDRs to effectively handle the residual LSI is discussed. These studies, and others similar works have mostly assumed (often implicitly) that the relay system has full-duplex capability, and the LSI can be eliminated perfectly. As a result, they not only lack actual implementation perspective, but also the strict potential requirements, such as synchronization of estimated LSI with additive looped SI, for effective real-time cancellation, while maintaining the feedback loop stability.

In contrast, this paper first analytically models both AF and DF relaying strategies in HD and FD modes, and then assesses their performances with a novel GNU Radio-based software

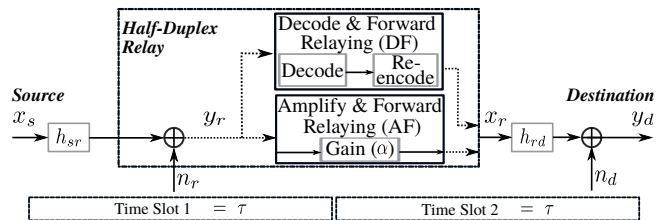


Figure 1. Block diagram of a two-hop transmission link communicating via an intermediary relay node operating in HD mode supporting both AF and DF relaying strategies.

implementation. Our solution for real-time simulative evaluation of FDR systems is based on open-source framework, and complies with IEEE 802.11a/g WLAN standard. Unlike the mentioned studies, our FDR implementation also allows to visualize the real-time LSI cancellation performance, its dependence on amplification factor and SI channel, and its resultant impact on SoI. Thus, providing fellow researchers a modular tool to further investigate and model the LSI behavior.

## III. MODELING OF RELAYING SYSTEM

In this work, we consider a two-hop relay system, where a source communicates with a destination via an intermediate relay node, which supports both AF and DF relaying strategies. In our framework, it is assumed that packets from the source cannot reach the destination directly, i.e., a non-cooperative decoding scheme, and the relay node in-between can operate in both HD and FD modes as shown in Figures 1 and 2, respectively.

### A. Half-Duplex Mode

When the considered system operates in HD transmission mode, depicted in Figure 1, the relay node receives a packet from source in time slot  $T_1$  and depending on the relaying strategy, either amplifies it by a factor  $\alpha$  or decodes and re-encodes it, before forwarding the packet towards destination in the next time slot  $T_2$ . The baseband samples at the inputs of relay ( $y_r$ ) and destination ( $y_d$ ) nodes can be written as

$$y_r[i] = x_s[i] * \bar{h}_{sr} + n_r[i], \quad (1)$$

$$y_d[i] = x_r[i] * \bar{h}_{rd} + n_d[i], \quad (2)$$

where  $x_s$  and  $x_r$  are the samples generated by source and relay nodes,  $n_r$  and  $n_d$  are the zero mean AWGN noise samples at the relay and destination ends, and  $\bar{h}_{sr}$ ,  $\bar{h}_{rd}$  are the channel impairment coefficients of source-relay and relay-destination channels, respectively. The instantaneous transmitted signal powers in Equations (1) and (2) can be obtained as  $E\{|x_s[i]|^2\} = P_s$  and  $E\{|x_r[i]|^2\} = P_r$ . Likewise, the noise powers at relay and destination nodes can be calculated as  $E\{|n_r[i]|^2\} = \sigma_r^2$  and  $E\{|n_d[i]|^2\} = \sigma_d^2$ .

1) *Amplify & Forward Relays:* In the case of AF relaying strategy, from (1) the instantaneous received SNR at relay node ( $\gamma_r$ ) can be computed as

$$\gamma_r = \frac{P_s \|h_{sr}\|^2}{\sigma_r^2}, \quad (3)$$

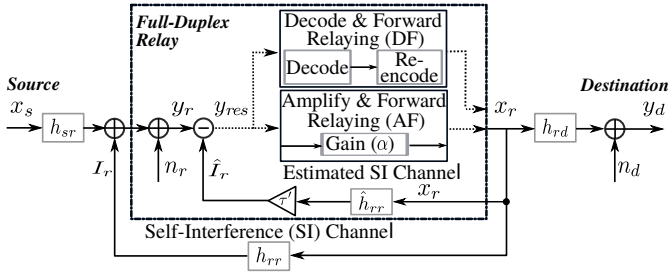


Figure 2. Block diagram of a two-hop transmission link communicating via an intermediary relay node operating in FD mode supporting both AF and DF relaying strategies.

where  $\|h_{sr}\|^2$  is the inner product of channel coefficients. In terms of source samples ( $x_s$ ), Equation (2) can be written as

$$y_d[i] = \alpha \cdot (x_s[i - \tau] * \bar{h}_{sr} + n_r[i - \tau]) * \bar{h}_{rd} + n_d[i], \quad (4)$$

where  $\tau$  is the delay of one time slot introduced before forwarding the samples towards destination. This delay basically prevents simultaneous transmission and reception that causes LSI (i.e., the full-duplex mode). Thus, from (4) the instantaneous end-to-end SNR ( $\gamma_d$ ) in AF-HDRs can be obtained as

$$\gamma_d = \frac{\alpha^2 \cdot P_s \|h_{sr}\|^2 \|h_{rd}\|^2}{\alpha^2 \cdot \sigma_r^2 \|h_{rd}\|^2 + \sigma_d^2}. \quad (5)$$

Using (3),  $\gamma_d$  in (5) can be obtained in terms of  $\gamma_r$  as

$$\gamma_d = \gamma_r \cdot \frac{\alpha^2 \cdot \|h_{rd}\|^2}{\alpha^2 \cdot \|h_{rd}\|^2 + \sigma_d^2 / \sigma_r^2}. \quad (6)$$

Hence, in (6),  $\gamma_d$  not only depends on the SNR acquired at relay node, but also on the amplification factor  $\alpha$ , and the ratio between noise powers of destination and relay ends.

2) *Decode & Forward Relays*: In the case of DF relaying strategy, from (1) the instantaneous received SNR at relay node ( $\gamma_r$ ) and destination node ( $\gamma'_d$ ) can be computed as

$$\gamma_r = \frac{P_s \|h_{sr}\|^2}{\sigma_r^2} \quad \text{and} \quad \gamma'_d = \frac{P_r \|h_{rd}\|^2}{\sigma_d^2}. \quad (7)$$

Since, DF relaying protocol decodes and re-encodes each symbol, therefore, the instantaneous end-to-end SNR ( $\gamma_d$ ) can be written as

$$\gamma_d = \min \left\{ \frac{P_s \|h_{sr}\|^2}{\sigma_r^2}, \frac{P_r \|h_{rd}\|^2}{\sigma_d^2} \right\}, \quad (8)$$

i.e.,  $\gamma_r$  or  $\gamma'_d$  whichever is the worst, benchmarks the overall DF-HDR performance.

### B. Full-Duplex Mode

When relaying is done in FD mode, the relay node receives the samples  $y_r$  from sources, and simultaneously forwards the processed samples  $x_r$  towards destination. This results in looped-back SI, which is therefore required to be suppressed before feeding the samples  $y_r$  to the amplification or decoding

blocks, as depicted in Figure 2. Otherwise, the DF protocol will not be able to decode anything, and the AF protocol will amplify and forward everything, including LSI.

The received samples at the input of a relay node after LSI suppression ( $y_{res}$ ) are obtained as

$$y_{res}[i] = x_s[i] * \bar{h}_{sr} + n_r[i] + I_r[i - \tau'] - \hat{I}_r[i - \tau']. \quad (9)$$

In (9),  $I_r$  and  $\hat{I}_r$  are the actual and estimated looped-back SI samples, and  $\tau'$  is the delay incurred by the channel and decoding process (DF strategy). Note that if  $\tau'$  is not acquired correctly, then the subtraction of non-synchronized estimated LSI  $\hat{I}_r$  from looped-back SI  $I_r$ , can drive the system towards instability. The residual signal samples ( $y_{res}$ ) in (9) can be reformulated as

$$y_{res}[i] = x_s[i] * \bar{h}_{sr} + n_r[i] + x_r[i - \tau'] * (\bar{h}_{rr} - \hat{h}_{rr}), \quad (10)$$

$$y_{res}[i] = x_s[i] * \bar{h}_{sr} + n_r[i] + x_r[i - \tau'] * \bar{e}_{rr}, \quad (11)$$

where  $\bar{h}_{rr}$  and  $\hat{h}_{rr}$  are the actual and estimated relay-relay channel coefficients, and  $\bar{e}_{rr}$  is the error between actual and estimated coefficients.

The received samples at the input of destination node ( $y_d$ ) are obtained as

$$y_d[i] = x_r[i] * \bar{h}_{rd} + n_d[i], \quad (12)$$

and the instantaneous transmitted signal power of the delayed sample can be computed as  $E\{|x_s[i - \tau']|^2\} = P'_s$  and  $E\{|x_r[i - \tau']|^2\} = P'_r$ .

1) *Amplify & Forward Relays*: From (11), the instantaneous SNR at relay node ( $\gamma_r$ ) after LSI suppression is obtained as

$$\gamma_r = \frac{P_s \|h_{sr}\|^2}{\sigma_r^2 + P'_r \|e_{rr}\|^2}, \quad (13)$$

where  $\|e_{rr}\|^2$  is the inner product of error vector. Note that the magnitude of residual LSI, i.e.,  $I_r - \hat{I}_r$ , increases with large  $\|e_{rr}\|^2$ , which eventually reduces the  $\gamma_r$ . From (11) and (12), the samples forwarded by relay node  $x_r$ , and the samples received at destination node  $y_d$  can be written as

$$x_r[i] = \alpha \cdot (x_s[i] * \bar{h}_{sr} + n_r[i] + x_r[i - \tau'] * \bar{e}_{rr}) \quad (14)$$

$$y_d[i] = \alpha \cdot (x_s[i] * \bar{h}_{sr} + n_r[i] + x_r[i - \tau'] * \bar{e}_{rr}) * \bar{h}_{rd} + n_d[i]. \quad (15)$$

Using (14),  $P'_r$  can be computed as

$$P'_r = \alpha^2 \cdot (P'_s \|h_{sr}\|^2 + \sigma_r^2 + P'_r \|e_{rr}\|^2), \quad (16)$$

and from (15), the instantaneous end-to-end SNR  $\gamma_d$  is obtained as

$$\gamma_d = \frac{\alpha^2 \cdot P_s \|h_{sr}\|^2 \|h_{rd}\|^2}{\alpha^2 \cdot \sigma_r^2 \|h_{rd}\|^2 + \alpha^2 \cdot P'_r \|e_{rr}\|^2 \|h_{rd}\|^2 + \sigma_d^2}. \quad (17)$$

Equation (17) can be rewritten in terms of  $\gamma_r$  as

$$\gamma_d = \gamma_r \cdot \frac{\alpha^2 \cdot \|h_{rd}\|^2}{\alpha^2 \cdot \|h_{rd}\|^2 (1 + P'_r \|e_{rr}\|^2 / \sigma_r^2) + \sigma_d^2 / \sigma_r^2}. \quad (18)$$

By analyzing (13), (16), and (18), it can be seen that the residual LSI due to  $\|e_{rr}\|^2$ , does not only have a direct impact on  $\gamma_d$ , but it also affects  $\gamma_d$  indirectly through  $\gamma_r$ .

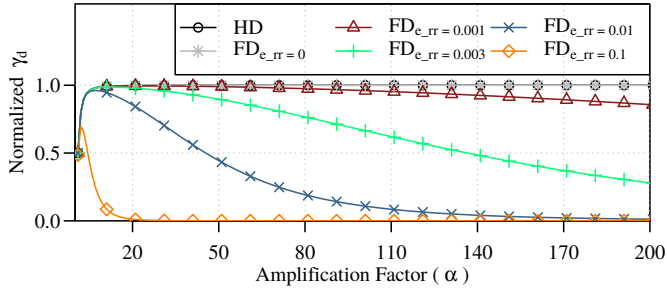


Figure 3. Instantaneous end-to-end SNR  $\gamma_d$  versus amplification factor  $\alpha$  for different  $\|e_{rr}\|^2$  values.

2) *Decode & Forward Relays*: In the case of DF relaying strategy, by using (11) and (12), the instantaneous received SNR at relay node ( $\gamma_r$ ) and destination node ( $\gamma'_d$ ) can be computed as

$$\gamma_r = \frac{P_s \|h_{sr}\|^2}{\sigma_r^2 + P_r' \|e_{rr}\|^2} \quad \text{and} \quad \gamma_d = \frac{P_r \|h_{rd}\|^2}{\sigma_d^2}, \quad (19)$$

and like DF-HDR, the instantaneous end-to-end SNR ( $\gamma_d$ ) in DF-FDR is obtained as

$$\gamma_d = \min \left\{ \frac{P_s \|h_{sr}\|^2}{\sigma_r^2 + P_r' \|e_{rr}\|^2}, \frac{P_r \|h_{rd}\|^2}{\sigma_d^2} \right\}. \quad (20)$$

From the comparison of (8) and (20) it can be seen that unlike HD mode,  $\gamma_d$  in FD mode is also affected by the residual LSI, i.e.,  $P_r' \|e_{rr}\|^2$  factor, and when  $\|e_{rr}\|^2 = 0$ , which in-practice never happens, both HD and FD modes offer same  $\gamma_d$ .

#### C. Impact of Amplification Factor on $\gamma_d$ in AF-based Relays

Unlike DF strategy, where the symbols are regenerated entirely at the relay node, in AF relaying the received samples are simply amplified and forwarded. Thus, for optimal performance, amplification factor plays a crucial role, especially in full-duplex mode where  $\alpha$  has a direct relation with error vector. Notice that for  $\|e_{rr}\|^2 = 0$  in (18), both HD and FD modes offer same  $\gamma_d$ .

Figure 3 shows the impact of amplification factor on received SNR  $\gamma_d$  for different  $\|e_{rr}\|^2$  values. For simplicity, all the other parameters in (18) are either normalized or set to 1. It can be seen in the plot that for a given  $\|e_{rr}\|^2$ ,  $\alpha$  provides an optimum  $\gamma_d$  at a certain value. Afterwards, it has no impact on  $\gamma_d$  in half-duplex mode; however, in full-duplex mode, large  $\alpha$  degrades the instantaneous SNR  $\gamma_d$ , where the degradation slope relies heavily on  $\|e_{rr}\|^2$ . These numerical results clearly show the critical dependence of AF-FDR performance on both amplification factor and error magnitude.

## IV. IMPLEMENTATION DETAILS

To evaluate the performance of both half-duplex and full-duplex transmission modes, we implemented the considered AF and DF relaying strategies in GNU Radio. We choose this platform because of its wide-spread use as a real-time signal processing framework and the rapid prototyping capabilities, supporting both simulation mode as well as experimental

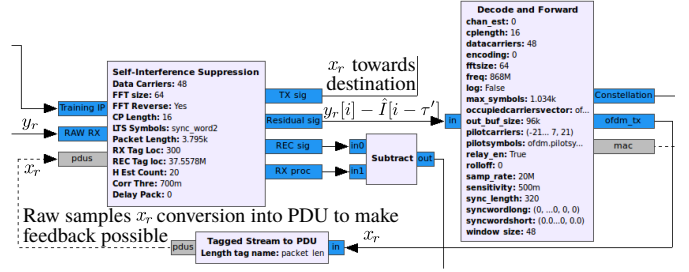


Figure 4. The most relevant blocks of our decode-and-forward based FDR implementation in GNU Radio Companion.

Table I  
Key physical layer parameters of the employed GNU Radio-based open source stack for IEEE 802.11a/g.

Parameters	
Modulations	B-PSK, Q-PSK, 16-QAM & 64-QAM
Code Rates	1/2, 3/4, 2/3
Sampling Frequency [MHz]	20
Data Rates [Mbit/s]	6, 9, 12, 18, 24, 36, 48, 54
FFT/IFFT Size	64 points
PLCP (Preamble + Header)	(12 + 1) OFDM Symbols

testing using Software Defined Radios (SDR). Additionally, the GNU Radio companion, a graphical tool for creating flow graph, allows to monitor the real-time received/processed samples through visualization scopes in both time and frequency domains. The GNU Radio implementation of our relaying system comprises of three parts:

(A) *Baseband Modulation/Demodulation*: For the baseband modulation/demodulation part, we used the GNU Radio-based open source stack for IEEE 802.11a/g/p WLAN developed by Bloessl et al. [8]. The core of this framework is a modular Orthogonal Frequency Division Multiplexing (OFDM) transceiver implementation, which is fully compatible with commercial WiFi cards, and has been thoroughly evaluated in [9]. The key physical layer parameters within this transceiver design are listed in Table I. One of the major reason of using this implementation is to later test our FD relaying system with SDR, and possibly evaluate its performance with commercial WiFi cards.

(B) *Channel Model*: For the performance evaluation of our relaying system under harsh channel conditions, we have implemented 6-taps frequency selective Rayleigh fading channels for both source-relay ( $h_{sr}$ ) and relay-destination ( $h_{rd}$ ) paths. Additionally, for LSI channel ( $h_{rr}$ ), a linear 3-taps fading channel is implemented. To keep  $h_{rr}$  more realistic, among the three taps first one is kept strongest as it maps the looped-back SI through direct path, and the remaining are kept weak to model the multi-path effect.

(C) *LSI Suppression*: For the cancellation of LSI, we have implemented a novel core block shown in Figure 4, which in the initial step transmits Long Training Sequence (LTS) symbols to estimate the SI channel ( $h_{rr}$ ), through time domain least square estimation as

$$\hat{h}_{rr} = \mathbf{X}^\dagger \cdot \bar{I}_{LTS}, \quad (21)$$

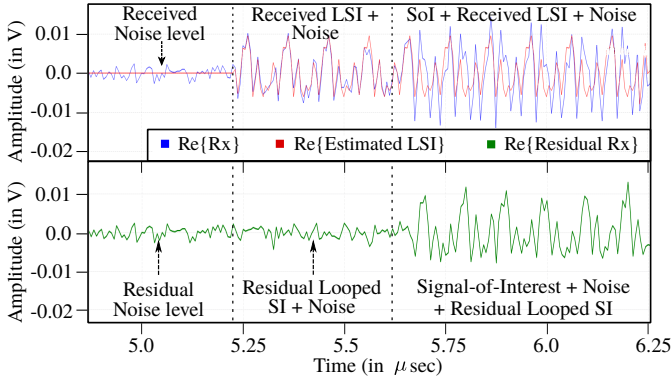


Figure 5. Snapshot of real-time LSI cancellation performance of our relay node in FD relaying mode.

where  $\mathbf{X}^\dagger$  denotes Moore-Penrose (pseudo) inverse of Toeplitz matrix  $\mathbf{X}$  formed through known LTS samples, and  $\tilde{I}_{LTS}$  are the received LTS samples. Further details on the estimation process can be found in [16]. Once the SI channel is estimated ( $\hat{h}_{rr}$ ), the LSI suppression block is all set to receive the actual samples  $y_r$ . The block first reconstructs the approximate LSI samples  $\hat{I}_r$  by using the estimate  $\hat{h}_{rr}$  and known  $x_r$ . It then buffers the reconstructed samples, to compensate for any delay  $\tau'$ , typically introduced by the SI channel and decoding process (DF strategy), and synchronizes  $I_r$  and  $\hat{I}_r$  based on a Start-of-Packet (SoP) indicator. Finally, it subtracts the delayed reconstructed samples from the received samples  $y_r$ , and forwards them either for amplification (AF case) or for decoding (DF case), as illustrated in Figure 2.

A screen shot of real-time looped-back SI cancellation performance at the relay node is shown in Figure 5. For the sake of clarity, the figure only shows the cancellation performance with real (in-phase) samples. The signals in blue, red, and green are received signal (including LSI), reconstructed LSI, and residual signal (after subtraction), respectively.

## V. PERFORMANCE EVALUATION

To draw a performance comparison between AF and DF relaying strategies in both HD and FD modes, we conducted an extensive set of real-time simulations. We investigated the impact of key parameters, i.e., the amplification factor and residual LSI, on the performance of our relaying system. We also computed the achievable spectral efficiency and physical layer latency of the implementation with each relaying strategy in both transmission modes.

In our simulation setup, we transmitted 100 packets for each Modulation and Coding Scheme (MCS) as listed in Table I, and measured the PDR based on received SNR. Each packet comprises of 250 B payload, 3 B header, and 4 B Cyclic Redundancy Check (CRC). For each SNR point, the packets transmission is repeated 20 times to obtain a 95% confidence interval, which for the sake of clarity is not shown in the plots. For fair comparison in both transmission modes, we empirically chose the optimum value of amplification factor ( $\alpha \approx 10$ ), and kept the average transmit power for path relay-destination same, i.e.,  $P_{\text{avg}}^{\text{AF}} \approx P_{\text{avg}}^{\text{DF}}$ , in both relaying strategies.

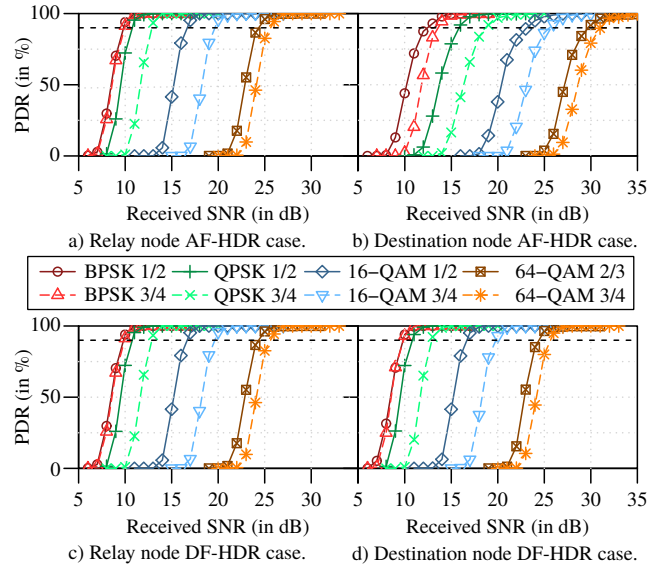


Figure 6. PDR versus received SNR at both relay and destination nodes, for  $\alpha \approx 10$  in Half-Duplex transmission modes.

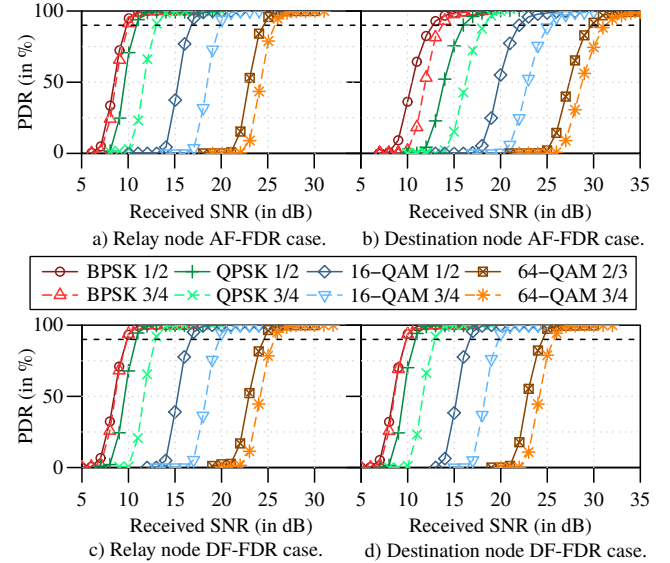


Figure 7. PDR versus received SNR at both relay and destination nodes, for  $\alpha \approx 10$  and residual LSI  $\approx -22$  dBm in Full-Duplex transmission modes.

### A. Packet Delivery Ratio: HDR vs. FDR

Figures 6 and 7 shows the PDR plots for each MCS at both relay and destination nodes for the two considered relaying strategies in HD and FD transmission modes, respectively. In all the plots, a PDR of 100% means that all packets have been correctly detected and decoded, and the horizontal dashed line marks 90% PDR. It is important here to mention that the PDR plots in Figure 7 (FD transmission mode), are obtained with non-negligible residual LSI.

From the comparison of Figure 6 (plots a & c) and Figure 7 (plots a & c), it can be seen that the 90% PDR performance of each MCS at the relay node in both AF and DF relaying strategies is roughly similar. There is a slightly degraded PDR

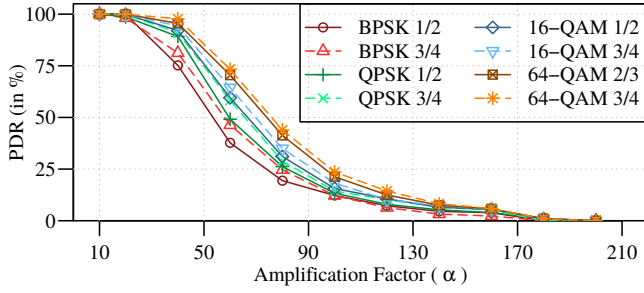


Figure 8. PDR versus amplification factor in AF-FDR case, with fixed relay SNR ( $\gamma_r$ ) and destination noise power ( $\sigma_d^2$ ).

performances in FD mode as compared to HD mode, certainly because of non-negligible residual looped-back SI in FD case. Additionally, within FD mode, the PDR performances with AF strategy is marginally lower than DF strategy. This is due to the negative impact of the amplification factor on the relay node received SNR, as studied in Section III-B.

Likewise, by comparing the PDR performances of each MCS at destination node, Figure 6 (plots b & d) and Figure 7 (plots b & d), we see that the AF relaying is performing roughly 6 dB–7 dB worse compared to DF relaying strategy. Even though the PDR performances with AF at relay node is rather similar to DF in both transmission modes, this is not the case at destination node. This performance drop is expected with AF relays because of their inherent dependence on amplification factor, which not only requires a critical selection, especially in FD case, but it also forwards the amplified noise component in the signal received at relay node.

1) *Impact of Amplification Factor in AF Relaying:* In Figure 8, the impact of amplification factor on the PDR of each MCS is plotted for AF-FDR case. It can be seen that for  $\alpha > 15$  the PDR of each MCS start decreasing drastically, and it more or less follow the same trend that we have already seen in the numerical plot shown in Figure 3. This is due to the reason that large  $\alpha$  intensifies the impact of residual looped SI, which not only reduces the SNR at destination node but it also negatively effects the SNR at relay node, as explained in Section III-B. Moreover, the PDR of lower order MCS seems to be affected more at larger  $\alpha$ , e.g., for BPSK 1/2. This is intuitive since the lower order MCS require low effective SNR to achieve high PDR, and a large amplification factor has a more adverse effect on already low  $\gamma_r$  and  $\gamma_d$ , which further aggravates the MCS performance.

2) *Impact of Residual Looped SI:* Figure 9 illustrates the impact of residual looped-back SI on the performance of each MCS in both AF and DF full-duplex relaying. The vertical-axis in the plot shows SNR levels required to maintain a 90% PDR at the relay node for exceeding levels of residual LSI over the noise floor. In the figure, we observe that when residual LSI surpasses the noise floor, more SNR is required to retain the 90% PDR. This is rather expected since looped-back SI is nothing but interference for the SoI, which means any residual LSI above the noise floor, basically reduces the

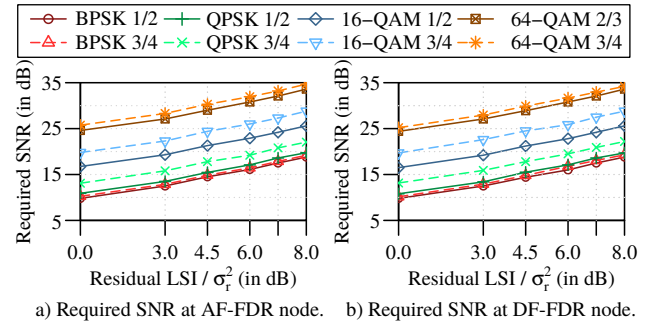


Figure 9. Required SNR level for each MCS to maintain 90% PDR with increasing levels of residual looped-back SI (for  $\alpha \approx 10$ ) at FDR node.

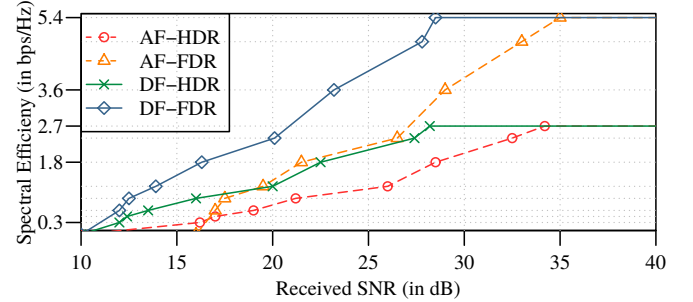


Figure 10. Spectral efficiency comparison with both AF and DF relaying strategies, operating in HD mode, and in FD mode with non-negligible residual LSI.

desired signal's SNR. Thus, in order to maintain the PDR performance, more SNR is required. Additionally, it can be noticed that the relation between required SNR and residual LSI is almost linear, take 64-QAM 3/4 as an example, where the required SNR raised from 25.5 dB–34.5 dB for an 8 dB gain of residual LSI over noise floor. This is due to the reason that the implemented LSI channel ( $h_{rr}$ ) has linear behavior, and therefore, the resultant LSI, and the residual LSI after suppression are also linear in nature.

### B. Achievable Spectral Efficiency: HDR vs. FDR

Figure 10 compares the achievable spectral efficiency in both HDR and FDR systems with increasing received SNR. In a typical IEEE 802.11a/g based HD systems, the maximum achievable spectral efficiency is 2.7 bps/Hz with 54 Mbit/s link. In our HDR implementation for IEEE 802.11a/g standard, the spectral efficiency improves with SNR, and it gets saturated at 2.7 bps/Hz with 64-QAM 3/4 MCS, i.e. 54 Mbit/s link, in both relaying strategies. Nevertheless, the AF relaying strategy requires roughly 6 dB–7 dB more SNR to attain similar bps/Hz as compared to DF relaying strategy.

In contrast, because of simultaneous reception and transmission capability of our FDR system, it is providing a two-fold increase in achievable spectral efficiency, i.e., 5.4 bps/Hz, with both relaying strategies. However, AF strategy needs an additional 7 dB SNR to reach the same bps/Hz performance as compared to DF strategy. Additionally, it can be gathered from the figure that for SNR levels up to 28 dB, it is better to use DF-HDR system because of its rather similar performance

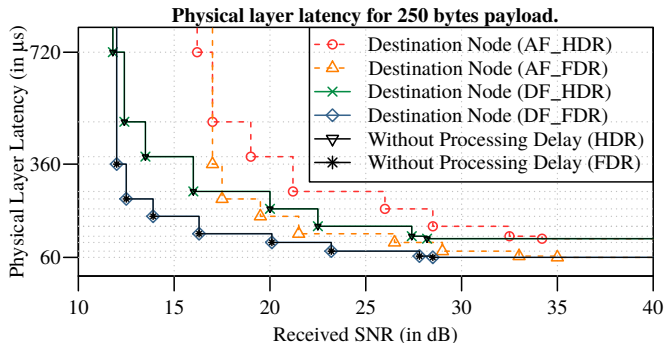


Figure 11. Physical layer latency comparison with both AF and DF (with and without decoding delay) relaying strategies, operating in half-duplex and full-duplex modes.

and relaxed processing requirements as compared to AF-FDR system. Moreover, if AF relaying is an absolute requirement, even then the deployment of AF-HDR is economically and performance-wise more beneficial for low data-rate links such as 6 Mbit/s and 9 Mbit/s as compared to AF-FDR system. In conclusion, DF-based FDR systems seems to be the ultimate choice with best bps/Hz performance, provided that the residual LSI is close to the noise floor.

### C. Physical Layer Latency (PLL): HDR vs. FDR

Figure 11 indicates the physical layer latencies introduced by each relaying strategy in both HD and FD transmission modes. Here, PLL is the time interval a payload engages while traversing from source to destination. In our relay system implementation, AF strategy does not introduce any delay in both HD and FD mode. However, due to the decoding and re-encoding process involved in DF strategy, a 150 ns delay is introduced in both modes, which is negligible compared to the considered payload size as can be seen in Figure 11.

Additionally, it can be noticed in the figure that AF relaying strategy in both HD and FD modes, requires roughly 7 dB more SNR to offer similar PLL performance as compared to its DF counterpart. Moreover, unlike the case of spectral efficiency, AF-FDR seems to completely outperform AF-HDR in-terms of low latency requirements. Nevertheless, DF-HDR is still offering better PLL as compared to AF-FDR at lower SNR levels of up-to 16.5 dB. In essence, DF-FDR outclassed all other relay implementations. For a 250 B payload, it landed-with the maximum latency of 360  $\mu$ s with the least SNR of 12.3 dB supporting 6 Mbit/s link only, and offered the best latency of 60  $\mu$ s at 28 dB SNR with a 54 Mbit/s link.

## VI. CONCLUSION

In this paper, we evaluated the performance of IEEE 802.11a/g compliant software-based Half-Duplex (HD) and Full-Duplex (FD) relay systems, with Amplify and Forward (AF) and Decode and Forward (DF) relaying strategies. By means of analytical modeling, we showed the critical dependence of AF relays on amplification factor, especially in FD transmission mode. Contrary to the earlier works, we further presented the real-time simulation results with our

GNU Radio-based implementation of the HD and FD relaying systems. Our results show the potential gains offered by FD relays in-terms of spectral efficiency and physical layer latency. In particular, given that the Looped Self-Interference (LSI) is sufficiently suppressed, DF-based Full-Duplex Relay (FDR) outclassed all other relaying systems.

Our IEEE 802.11a/g compliant FDR implementation is based on open-source GNU Radio framework, which supports both simulation modeling and experimental testing through Software Defined Radios (SDR). With successful simulative evaluation, in future, we plan to analyze the performance of our FDR implementation with SDR, and possibly with other WiFi cards.

## REFERENCES

- [1] 3GPP, "Further advancements for E-UTRA physical layer aspects," 3GPP, TR 36.814 V9.0.0 (2010-03), Mar. 2010.
- [2] "Local and metropolitan area networks," IEEE, Standard P802.16j-06/026r4, May 2007.
- [3] Z. Zhang, K. Long, A. V. Vasilakos, and L. Hanzo, "Full-duplex wireless communications: Challenges, solutions, and future research directions," *Proceedings of the IEEE*, vol. 104, no. 7, pp. 1369–1409, 2016.
- [4] D. Bharadia, E. McMillin, and S. Katti, "Full Duplex Radios," *ACM SIGCOMM Computer Communication Review (CCR)*, vol. 43, no. 4, pp. 375–386, Oct. 2013.
- [5] E. Ahmed and A. M. Eltawil, "All-digital self-interference cancellation technique for full-duplex systems," *IEEE Transactions on Wireless Communications*, vol. 14, no. 7, pp. 3519–3532, 2015.
- [6] M. S. Amjad, H. Nawaz, K. Ozsoy, O. Gurbuz, and I. Tekin, "A Low-Complexity Full-Duplex Radio Implementation With a Single Antenna," *IEEE Transactions on Vehicular Technology*, vol. 67, no. 3, pp. 2206–2218, Mar. 2018.
- [7] J. Zhou, N. Reiskarimian, J. Diakonikolas, T. Dinc, T. Chen, G. Zussman, and H. Krishnaswamy, "Integrated Full Duplex Radios," *IEEE Communications Magazine*, vol. 55, no. 4, pp. 142–151, 2017.
- [8] B. Bloessl, M. Segata, C. Sommer, and F. Dressler, "An IEEE 802.11a/g/p OFDM Receiver for GNU Radio," in *ACM SIGCOMM 2013, 2nd ACM SIGCOMM Workshop of Software Radio Implementation Forum (SRIF 2013)*. Hong Kong, China: ACM, Aug. 2013, pp. 9–16.
- [9] —, "Performance Assessment of IEEE 802.11p with an Open Source SDR-based Prototype," *IEEE Transactions on Mobile Computing*, vol. 17, no. 5, pp. 1162–1175, May 2018.
- [10] J. Laneman, D. Tse, and G. Wornell, "Cooperative Diversity in Wireless Networks: Efficient Protocols and Outage Behavior," *IEEE Transactions on Information Theory*, vol. 50, no. 12, pp. 3062–3080, Dec. 2004.
- [11] B. Rankov and A. Wittneben, "Spectral efficient protocols for half-duplex fading relay channels," *IEEE Journal on Selected Areas in Communications*, vol. 25, no. 2, pp. 379–389, Feb. 2007.
- [12] J. Jiao, X. Jia, M. Zhou, M. Xie, and Q. Cao, "Full-duplex massive MIMO AF relaying system with low-resolution ADCs under ZFT/ZFR scheme," in *2nd IEEE Advanced Information Technology, Electronic and Automation Control Conference (IAEAC 2017)*. Chongqing, China: IEEE, Mar. 2017, pp. 2024–2028.
- [13] Q. Li, S. Feng, X. Ge, G. Mao, and L. Hanzo, "On the Performance of Full-Duplex Multi-Relay Channels With DF Relays," *IEEE Transactions on Vehicular Technology*, vol. 66, no. 10, pp. 9550–9554, Oct. 2017.
- [14] T.-C. Chen, Y.-C. Chen, M.-K. Chang, and G.-C. Yang, "The Impact of Loopback Channel Estimation Error on Performance of Full-Duplex Two-Way AF Relaying Communication Systems," in *85th IEEE Vehicular Technology Conference (VTC2017-Spring)*. Sydney, Australia: IEEE, Jun. 2017.
- [15] L. Elsaid, M. Ranjbar, N. Raymondi, D. Nguyen, N. Tran, and A. Mahamadi, "Full-Duplex Decode-and-Forward Relaying: Secrecy Rates and Optimal Power Allocation," in *85th IEEE Vehicular Technology Conference (VTC2017-Spring)*. Sydney, Australia: IEEE, Jun. 2017.
- [16] M. S. Amjad and O. Gurbuz, "Linear Digital Cancellation with Reduced Computational Complexity for Full-Duplex Radios," in *IEEE Wireless Communications and Networking Conference (WCNC 2017)*. San Francisco, CA: IEEE, Mar. 2017.